

The unusual quadruple system HD 91962 with a “planetary” architecture

Andrei Tokovinin

Cerro Tololo Inter-American Observatory, Casilla 603, La Serena, Chile
 atokovinin@ctio.noao.edu

David W. Latham

Harvard-Smithsonian Center for Astrophysics, 60 Garden Street, Cambridge, MA 02138, USA
 dlatham@cfa.harvard.edu

Brian D. Mason

U.S. Naval Observatory, 3450 Massachusetts Ave., Washington, DC, USA
 bdm@usno.navy.mil

ABSTRACT

The young nearby solar-type star HD 91962 is a rare quadruple system where three companions revolve around the main component with periods of 170.3 days, 8.84 years, and 205 years. The two outer orbits are nearly co-planar, and all orbits have small eccentricities. We refine the visual orbit of the outer pair, determine the combined spectro-interferometric orbit of the middle 8.8-yr pair and the spectroscopic orbit of the inner binary. The middle and inner orbits are likely locked in a 1:19 resonance, the ratio of the outer and middle periods is ~ 23 . The masses of all components are estimated (inside-out: 1.14, 0.32, 0.64, 0.64 solar mass), the dynamical parallax is 27.4 ± 0.6 mas. We speculate that this multiple system originated from collapse of an isolated core and that the secondary components migrated in a dissipative disk. Other multiple systems with similar features (coplanarity, small eccentricity, and period ratio around 20) are known.

Subject headings: stars: binaries

1. System description

The observed architectures of stellar systems depend both on the formation processes and subsequent evolution. In many cases the orbits preserve information about the formation processes, and their study helps us to understand the physics of fragmentation, accretion, and early evolution of stars. This information is gleaned from observations of young binaries, from statistics of binary and multiple stars in different environments (Duchêne & Kraus 2013), and from unusual objects that reveal the history of their formation like “Rosetta stones”. One such object is featured

here.

The 7th magnitude G1V star studied here is known as HD 91962, HIP 51966, WDS J10370–0850, or ADS 7854; the J2000 coordinates are 10:37:00.01, –08:50:23.7. It is located at a distance of 36 pc from the Sun. HD 91962 is an X-ray source RX J1036.9–0850 and a hierarchical quadruple system (Figure 1).

The outer binary A,B (A 556) is known since 1903 (Aitken 1904). Its orbit with $P = 283$ yr by Popovic (1978) was recently revised by Tokovinin et al. (2014). We show below that the period is close to 200 yr. The original *Hipparcos* parallax is 27.5 ± 1.3 mas, the new *Hippar-*

cos reduction (van Leeuwen 2007) revised it to 25.1 ± 1.2 mas. However, the *Hipparcos* parallax could be biased by the orbital motion which was not taken into consideration in its data reduction.

The subsystem Aa,Ab (TOK 44) was discovered by Metchev & Hillenbrand (2009) with adaptive optics in 2003.354, at $0^{\circ}142$, $56^{\circ}2$, $\Delta K = 1.25$ mag. Independently, it was resolved in 2009 by speckle interferometry at SOAR (Tokovinin et al. 2010) and was measured several times since then. The pair Aa,Ab was seen in 2012.18 at the same position as in 2003.35, completing one full revolution. The orbital period is therefore well constrained by the speckle measurements.

DL independently determined the spectroscopic orbit of Aa,Ab with a period of 3233 ± 20 days (8.85 yr) and discovered the inner spectroscopic subsystem Aa1,Aa2 with $P = 170.3$ d. This is therefore a hierarchical quadruple system with a 3-tier “planetary” architecture, where all components revolve around the most massive central star Aa1. The two inner orbits have small and similar eccentricities and their apsidal angles are also similar. We show below that these orbits are locked in a 1:19 mutual resonance. The period of the outer visual orbit is about 20 times longer than the period of the middle orbit.

The observational material is presented in Section 2. It is used for calculation of the orbits

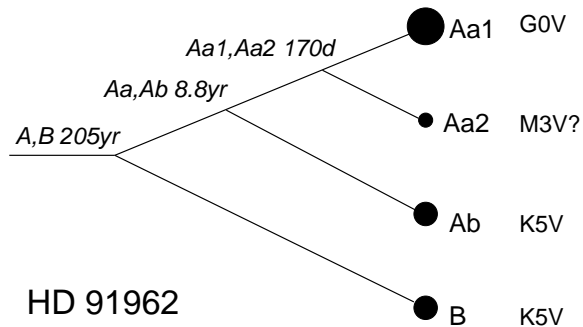


Fig. 1.— Structure of the hierarchical quadruple system HD 91962. Components are designated by letters and numbers, subsystems are identified by their components joined by the comma. Approximate spectral types are assigned to match the estimated masses of the stars. All orbits have small eccentricity and are possibly located in one plane.

in Section 3 and for the estimate of component’s masses and distance to the system (Section 4). In Section 5 we discuss the formation mechanism of such hierarchies and give examples of other 3-tier hierarchical systems with known orbits.

2. Observations

2.1. Speckle interferometry

All resolved measurements of the middle subsystem Aa,Ab except the first one come from the 4.1-m SOAR telescope. The instrument and data reduction are described by Tokovinin et al. (2010). The observations were made with the 534/22 nm interference filter close to the Strömgren y band and the 788/132 nm filter approximating the Cousins system I_C . Figure 2 presents samples of the speckle auto-correlation functions (ACFs) of the resolved triple star. The relative position and brightness of the components is determined by least-squares fitting of the power spectrum to a triple-star model (not from the ACF). The orientation of the inner pair is determined without the usual 180° ambiguity when the correlation peak between Ab and B is detectable (it is barely seen in the y filter). Three observations made in 2014 are still unpublished. After submission of the manuscript, two more measurements made in 2015 were added, slightly reducing the errors of the middle orbit. We also use one unpublished measure of A,B made in 2001 by BM (the subsys-

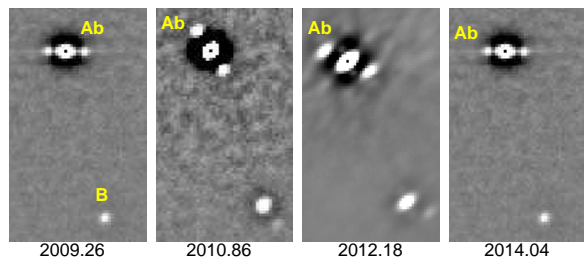


Fig. 2.— Fragments of speckle auto-correlation functions showing the resolved triple system. The scale and orientation are approximate (North up, East left). The two middle images (2010.86 and 2012.18) are taken in the I_C band and contain the faint peak corresponding to the cross-correlation between B and Ab. In the remaining images (in the y filter) this peak is lost in the noise.

tem was not resolved).

2.2. Spectroscopy

The spectrum of HD 91962 was monitored for 23 years starting in 1991. Eighty-four observations were obtained with the CfA Digital Speedometers (Latham 1985, 1992), initially using the 1.5-m Wyeth Reflector at the Oak Ridge Observatory in the town of Harvard, Massachusetts, and subsequently with the 1.5-m Tillinghast Reflector at the Whipple Observatory on Mount Hopkins, Arizona. Starting in 2009 the new fiber-fed Tillinghast Reflector Echelle Spectrograph (TRES; Szentgyorgyi & Furész 2007) was used to obtain an additional ten observations. The spectral resolution was 44,000 for all three spectrographs, but the typical signal-to-noise ratio (SNR) per resolution element of 100 for the TRES observations was a few times higher than for the CfA Digital Speedometer observations.

The total light of HD 91962 is dominated by the component Aa1, and at visible wavelengths the spectrum appears single-lined. Therefore we followed our standard procedure of using one-dimensional correlations of each observed spectrum against a synthetic template drawn from our library of calculated spectra. The radial velocity (RV) zero point for each spectrograph was monitored using observations of standard stars, of day-time sky, and of minor planets, and the velocities were all adjusted to the native system of the CfA Digital Speedometers. To get onto the absolute velocity system defined by our observations of minor planets, about 0.14 km s^{-1} should be added to the velocities reported in Table 3. These velocities are all based on correlations of just a single echelle order centered on the Mg b triplet near 519 nm, with a wavelength window of 4.5 nm for the CfA Digital Speedometers and 10.0 nm for TRES.

The ten TRES observations were analyzed with the Stellar Parameter Classification tool (SPC; Buchhave et al. 2014). The results are given in Table 1. As they are mutually consistent, we list the average values of stellar parameters and their errors estimated from the scatter of ten measurements. The parameters found in the literature are given for comparison. The star Aa1 dominates in the visible light, with all other components together contributing only 14%. Therefore their influence on the derived stellar parameters of Aa1 is

minor.

2.3. Photometry

Table 2 gathers the photometric information. Its column (2) gives the combined magnitudes of AB, with V from SIMBAD, I_C calculated from the $V - I$ color given in (van Leeuwen 2007), and K_s from 2MASS (Cutri et al. 2003). The magnitude differences between Ab and Aa and between B and A are given in the columns (3) and (4). They are based on speckle interferometry at SOAR, assuming $\Delta V \approx \Delta y$, and on photometry from (Metchev & Hillenbrand 2009): $\Delta K_{Aa,Ab} = 1.25 \pm 0.11 \text{ mag}$ and $\Delta K_{AB} = 1.37 \pm 0.06 \text{ mag}$. The scatter of the relative speckle photometry is about 0.1 mag, and the magnitude difference between Aa and B is slightly over-estimated owing to the anisoplanatism. This bias is overcome by using the relative photometry of the wide pair on the long-exposure images produced from the speckle data cubes: $\Delta y_{AB} = 2.67 \pm 0.10 \text{ mag}$ and $\Delta I_{AB} = 2.09 \pm 0.05 \text{ mag}$, in good agreement with *Hipparcos* and *Tycho* (Fabricius & Makarov 2000): $\Delta H_{pAB} = 2.69$, $\Delta V_{AB} = 2.48$ and $\Delta B_{AB} = 3.30 \text{ mag}$. Note also the magnitude difference $\Delta V_{AB} = 2.52 \text{ mag}$ measured by Horch et al. (2001).

The last three columns of Table 2 list individual magnitudes calculated from the combined and differential photometry. The component Aa is treated as a single star, while it is in fact a 170-d binary. Masses given in the last line are discussed in Section 4.

3. Orbits

Table 3 lists the orbital elements and their errors for all three orbits: outer, middle, and inner. In purely visual orbits, the ascending node is not known, meaning that both elements Ω and ω can be changed by 180° . Radial velocities help to select the correct node. Here the longitude of periastron ω_A corresponds to the primary component, and the position angle of the node Ω_A is chosen in such way as to represent the motion of the secondary on its visual orbit. Estimated or assumed quantities are given in brackets for reference. The orbital elements and their errors are determined by the unconstrained least-squares fit to the data (RVs, positional measurements, or both) with weights inversely proportional to the squares

TABLE 1
PARAMETERS OF THE STAR Aa1

T_e (K)	$\log g$ (m s^{-2})	[m/H] (Sun)	$V \sin i$ km s^{-1}	Reference
5827	4.49	-0.15	9.27	This work
± 17	± 0.01	± 0.01	± 0.26	
5818	4.85	...	6.10	Schroeder et al. (2009)
5675	4.12	-0.21	...	Casagrande et al. (2011)

TABLE 2
PHOTOMETRY OF COMPONENTS

Band	A+B	Ab-Aa	B-A	Aa	Ab	B
V (mag)	7.03	2.86 ± 0.10	2.67 ± 0.10	7.19	10.05	9.80
I_C (mag)	6.34	2.29 ± 0.10	2.09 ± 0.05	6.62	8.91	8.55
K_s (mag)	5.39	1.25 ± 0.11	1.37 ± 0.06	5.96	7.21	7.03
Mass (\mathcal{M}_\odot)	2.74	1.46	0.64	0.64

TABLE 3
ORBITAL ELEMENTS OF HD 91962.

Element	A,B	Aa,Ab	Aa1,Aa2
P (yr)	205 (fixed)	8.84638 ± 0.025	0.46628 ± 0.00005
P (d)	74875 (fixed)	3230.8 ± 9	170.304 ± 0.013
T (yr)	2048.6 ± 2.5	2009.816 ± 0.072	2003.292 ± 0.005
T (JD + 2,400,0000)	69290 ± 873	55129 ± 26	52746.80 ± 1.48
e	0.301 ± 0.016	0.125 ± 0.010	0.135 ± 0.008
a (arcsec)	1.334 ± 0.016	0.1501 ± 0.0021	(0.0184)
Ω_A (deg)	63.2 ± 2.0	50.4 ± 1.0	...
ω_A (deg)	219.7 ± 1.3	263.9 ± 2.6	297.6 ± 3.2
i (deg)	54.2 ± 0.8	56.6 ± 0.9	(57)
K_1 (km s^{-1})	(0.21)	4.71 ± 0.07	8.08 ± 0.07
V_0 (km s^{-1})	21.16 ± 0.04

TABLE 4
RADIAL VELOCITIES AND RESIDUALS

JD +2,400,000	RV (km s ⁻¹)	Err (km s ⁻¹)	O-C (km s ⁻¹)	JD +2,400,000	RV (km s ⁻¹)	Err (km s ⁻¹)	O-C (km s ⁻¹)
48290.835	12.11	0.44	0.35	53838.722	19.32	0.21	-0.07
49051.810	28.68	0.43	-0.35	53866.741	13.20	0.19	-0.32
49165.488	27.95	0.39	0.22	53871.656	12.16	0.25	-0.63
49384.843	32.55	0.32	0.64	54071.034	10.39	0.23	-0.39
49391.711	31.52	0.39	1.09	54077.023	11.65	0.20	0.05
49479.349	19.67	0.41	-0.03	54100.952	18.56	0.25	-0.22
49480.348	19.75	0.42	-0.14	54107.933	21.17	0.22	-0.21
49483.360	20.42	0.37	-0.12	54127.920	25.35	0.36	-0.56
49708.698	34.25	0.49	0.68	54135.897	26.03	0.21	0.07
49748.613	25.63	0.41	-0.05	54158.887	22.25	0.18	-0.03
49750.574	25.13	0.37	-0.07	54166.821	20.25	0.25	-0.15
49775.520	20.33	0.55	0.48	54187.787	15.59	0.28	0.22
49807.431	16.69	0.41	-0.48	54192.724	13.92	0.42	-0.36
49813.412	17.03	0.45	-0.56	54196.739	12.68	0.27	-0.77
50070.693	27.17	0.41	-1.03	54221.689	10.57	0.24	0.76
50128.539	16.18	0.43	0.21	54251.721	11.73	0.28	0.08
50138.507	15.10	0.49	-0.04	54277.656	20.74	0.29	0.35
50161.454	16.20	0.36	-0.37	54457.972	22.99	0.21	-0.12
50163.476	17.20	0.38	0.23	54461.968	25.02	0.23	1.05
50170.394	18.79	0.49	0.05	54481.934	24.54	0.23	0.08
50183.390	22.96	0.38	-0.29	54486.927	24.67	0.22	0.88
50185.384	23.89	0.43	-0.12	54516.861	17.48	0.23	0.26
50189.385	25.06	0.45	-0.44	54521.883	16.28	0.35	0.24
50458.658	15.34	0.37	0.27	54543.743	11.82	0.29	0.30
50460.619	15.59	0.43	0.84	54549.829	10.93	0.25	0.37
50484.559	12.56	0.44	-0.02	54576.693	8.38	0.22	-0.62
50514.480	17.80	0.42	0.41	54601.702	14.80	0.32	0.91
50516.461	18.47	0.43	0.42	54605.617	15.23	0.35	-0.04
52997.868	21.85	0.28	-0.67	54808.035	25.21	0.22	-0.53
53037.771	17.90	0.32	0.83	54839.907	22.61	0.29	-0.02
53054.679	18.59	0.27	0.29	54846.883	20.91	0.22	-0.16
53087.635	28.91	0.35	0.21	54868.897	16.35	0.22	0.28
53106.657	33.38	0.34	0.65	54878.903	13.67	0.26	-0.41
53353.876	17.92	0.28	0.46	54898.830	10.77	0.28	-0.48
53388.852	15.65	0.36	0.29	54924.741	11.15	0.30	-0.46
53403.862	18.33	0.22	0.29	54957.690	22.20	0.30	0.38
53418.705	23.45	0.23	0.43	54962.655	23.28	0.31	-0.35
53433.695	27.45	0.27	-0.78	55169.033	28.08	0.10	-0.25
53448.694	30.38	0.26	-0.21	55172.031	27.66	0.10	-0.18
53465.621	28.12	0.46	-1.14	56743.750	19.17	0.10	-0.31
53485.588	24.59	0.26	-0.31	56790.638	13.60	0.10	-0.23
53510.706	19.19	0.19	0.29	56804.634	15.39	0.10	-0.14
53541.647	14.13	0.26	0.05	56811.653	17.16	0.10	-0.09
53721.004	12.61	0.52	0.07	56817.658	19.05	0.10	-0.10
53746.976	16.04	0.33	-0.27	56820.637	19.99	0.10	-0.21
53776.914	26.13	0.45	-0.34	56825.656	22.02	0.10	-0.06
53836.847	19.84	0.21	0.00	56827.656	22.60	0.10	-0.23

TABLE 5
MEASUREMENTS AND RESIDUALS OF Aa,Ab

Date	θ (deg)	ρ (arcsec)	σ_ρ (arcsec)	$(O-C)_\theta$ (deg)	$(O-C)_\rho$ (arcsec)
2003.354	56.2	0.142	0.005	-2.5	-0.009
2009.263	268.8	0.097	0.005	0.1	0.000
2010.969	29.0	0.122	0.005	1.6	0.003
2010.969	30.0	0.125	0.005	2.5	0.006
2012.184	58.0	0.151	0.005	-0.3	0.000
2012.184	58.1	0.151	0.005	-0.2	0.000
2013.132	81.9	0.124	0.005	0.1	-0.005
2013.132	83.8	0.135	0.105	1.9	0.006
2014.043	117.7	0.097	0.002	-1.1	0.000
2014.186	126.6	0.097	0.002	0.1	0.003
2014.300	133.0	0.097	0.002	0.0	0.004
2015.029	172.1	0.098	0.002	-0.9	-0.005
2015.169	181.0	0.108	0.002	1.6	0.001

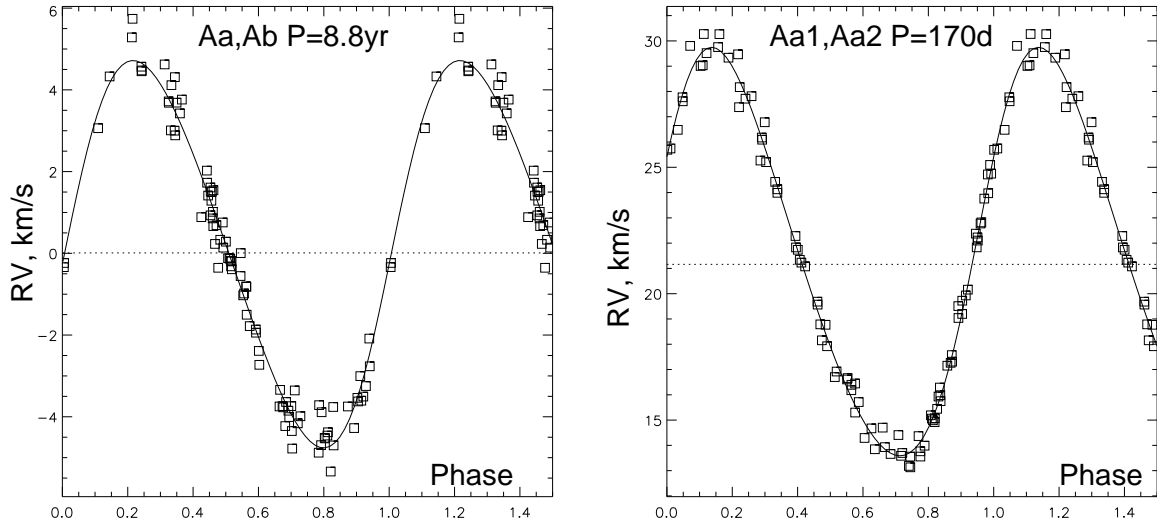


Fig. 3.— Spectroscopic orbits of the middle (left) and the inner (right) subsystems of HD 91962.

TABLE 6
MEASUREMENTS AND RESIDUALS OF A,B

Date	θ (deg)	ρ (arcsec)	σ_ρ (arcsec)	(O-C) $_\theta$ (deg)	(O-C) $_\rho$ (arcsec)
1903.040	54.0	1.340	0.500	-5.3	-0.185
1909.320	65.2	1.800	0.100	1.4	0.214
1909.320	65.0	1.640	0.100	1.2	0.054
1911.100	60.4	1.600	0.100	-4.6	0.001
1912.046	66.2	1.650	0.100	0.6	0.045
1915.210	69.6	1.480	0.100	1.8	-0.140
1916.210	70.0	1.700	0.100	1.6	0.076
1921.360	73.1	1.610	0.100	1.3	-0.023
1925.340	76.8	1.680	0.100	2.4	0.050
1926.260	77.0	1.550	0.100	2.0	-0.078
1928.160	81.3	1.520	0.100	5.0	-0.102
1929.510	74.2	1.540	0.100	-3.0	-0.077
1933.280	78.0	1.560	0.100	-1.7	-0.038
1933.960	76.5	1.330	0.500	-3.7	-0.264
1936.250	81.4	1.350	0.100	-0.4	-0.228
1939.300	81.5	1.520	0.100	-2.4	-0.034
1944.010	86.4	1.450	0.100	-1.0	-0.059
1944.290	92.4	1.400	0.100	4.7	-0.106
1947.930	89.0	1.280	0.100	-1.5	-0.184
1956.340	97.6	1.280	0.100	-0.3	-0.074
1957.760	106.2	1.520	0.100	6.9	0.187
1958.000	97.0	1.420	0.100	-2.5	0.091
1958.040	103.1	1.380	0.100	3.5	0.051
1959.160	110.8	1.600	1.100	10.1	0.285
1959.300	97.7	1.140	0.100	-3.1	-0.170
1962.500	110.3	1.180	0.100	6.1	-0.082
1966.380	108.4	1.200	0.100	-0.3	-0.002
1972.112	116.5	1.140	0.100	0.4	0.026
1972.120	113.1	0.920	0.100	-3.0	-0.194
1977.280	121.3	1.160	0.100	-2.6	0.123
1982.260	127.9	1.010	0.100	-4.1	0.039
1991.250	151.7	0.886	0.010	0.7	0.001
1996.350	141.7	0.723	1.100	-21.0	-0.138
1997.123	165.6	0.833	0.020	1.1	-0.027
1997.300	141.4	0.753	1.100	-23.5	-0.106
2001.077	172.4	0.842	0.005	-1.5	-0.017
2002.167	177.3	0.873	0.005	0.9	0.012
2009.263	192.6	0.906	0.005	0.0	0.013
2010.969	196.0	0.899	0.005	-0.3	-0.006
2010.969	196.0	0.904	0.005	-0.3	-0.001
2012.184	198.7	0.909	0.005	-0.2	-0.005
2013.132	200.7	0.924	0.005	-0.0	0.004
2013.132	200.9	0.926	0.005	0.1	0.006
2014.043	203.1	0.923	0.005	0.4	-0.005
2014.186	202.9	0.925	0.005	-0.1	-0.003
2014.300	203.5	0.933	0.005	0.3	0.004
2015.029	204.7	0.939	0.005	-0.0	0.004
2015.169	205.4	0.937	0.005	0.4	0.001

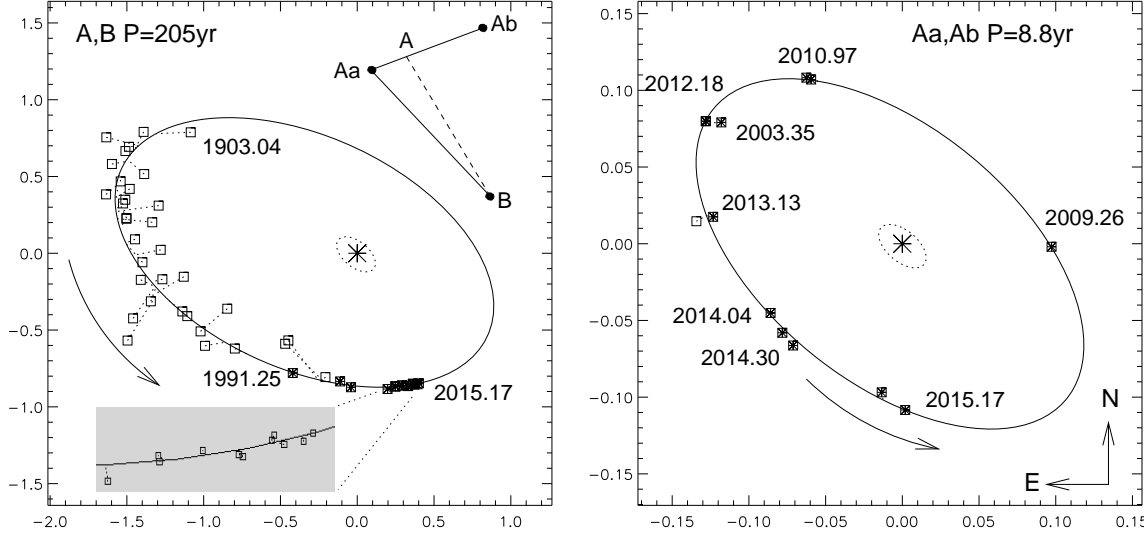


Fig. 4.— Visual orbits of the outer system A,B (left) and the middle system Aa,Ab (right). The scale is in arcseconds. The small dotted ellipses shows inner orbits to scale (Aa1,Aa2 is assumed to be co-planar with Aa,Ab). The scheme in the left panel illustrates the correction of the resolved measurements of Aa,B using the vector formula $Aa, B = Aa, A + A, B$.

of the measurement errors. The center-of-mass velocity is common to all three orbits, but we do not know yet the spectroscopic elements of A,B and arbitrarily ascribe V_0 to the inner pair Aa1,Aa2 meanwhile.

The RVs used in the orbit calculation and common residuals to the orbits of Aa1,Aa2 and Aa,Ab are presented in Table 4. The speckle measurements of Aa,Ab and residuals to its orbit are listed in Table 5. The first measurement is made by Metchev & Hillenbrand (2009), all remaining measurements are made at SOAR.

The orbit of the middle pair Aa,Ab was initially determined independently from both speckle interferometry and RVs. We used the initial spectroscopic orbits of Aa,Ab and Aa1,Aa2 fitted jointly to the RV data alone as a first approximation to the combined orbit of Aa,Ab (the 170-d orbit was then subtracted from the RVs). With this combined solution, another iteration on the inner system was made, giving essentially the same elements. The weighted rms RV residual to both orbits is 0.42 km s^{-1} . Figure 3 shows the RV curves, while Figure 4 shows the visual orbits of Aa,Ab and A,B.

The final elements of Aa,Ab and their errors are determined by the least-squares fit to both RVs and resolved measures. The speckle errors are assumed to be 5 mas prior to 2014 (except for one less precise measure). and 2 mas for 2015–2015. The rms residuals are 1.2 and 3.4 mas in θ and ρ , respectively. We had to adopt realistic speckle errors (hence weights) to reach the correct balance between positional measurements and RVs. The formal errors delivered by the speckle data processing are smaller, typically under 1 mas.

We updated the visual orbit of the outer system A,B = A 556 (see the elements in Table 3, observations and residuals in Table 6). The speckle measures of Aa,B (all data from SOAR where the triple is resolved) are translated into the positions of A,B, where A refers to the center of mass of Aa,Ab. The position of the inner pair Aa,Ab was calculated from its known orbit and the vector directed from Aa to Ab was added to the vector Aa,B with a coefficient $\alpha = -q/(1+q) = -0.305$ ($q = 0.44$ is the mass ratio in Aa,Ab). The unresolved accurate measurements (1991–2001) were corrected with $\alpha = -(q-r)/[(1+q)(1+r)] = -0.237$, considering that they refer to the photocenter of Aa,Ab and not to A or Aa ($r = 0.07$ is the

light ratio Ab/Aa). This correction substantially reduces the scatter of accurate speckle measurements (see the scheme and the zoomed portion of the orbit in Figure 4, left). The visual micrometer measurements are left uncorrected, as the effect of Aa, Ab is < 36 mas. They are assigned errors of $0''.1$, except the four highly deviant micrometer measurements that were given larger errors to cancel their influence on the orbit.

It turns out that the data do not yet constrain all elements of the outer pair A,B. Equally good solutions can be obtained by fixing the period at different values within a certain range; longer periods correspond to a smaller mass sum. The orbit given here assumes $P = 205$ yr and gives the mass sum of $2.68 M_{\odot}$ for a parallax of 27.6 mas. The unconstrained fit gives $P = 240 \pm 35$ years.

Using the masses estimated below, we calculate that the RV amplitude in the A,B orbit is $K_1 = 0.2 \text{ km s}^{-1}$. The ephemeris predicts that the $RV(A)$ should change by -0.18 km s^{-1} during the period 1991–2014 covered by the observations. We fitted the RV residuals by a linear function and found the coefficient of $-0.007 \pm 0.008 \text{ km s}^{-1} \text{ yr}^{-1}$, or a total change of -0.17 km s^{-1} during the 23-yr period of RV observations. The coincidence of those numbers is accidental, given that the RV trend is not formally significant. However, the *sign* of the emerging RV trend tells us that the node of the orbit of A,B is probably chosen correctly. Therefore, the orbits of A,B and Aa,Ab are nearly co-planar (the angle between the angular momenta is $\phi = 10.8^{\circ} \pm 1.9^{\circ}$). If the node of the outer orbit is changed by 180° , then $\phi = 110^{\circ}$. In such case, the Kozai-Lidov cycles would have made the middle orbit highly eccentric and would have destroyed the architecture of this multiple system.

The calculated semi-major axis of Aa1,Aa2 is 18.4 mas. The “wobble” of Aa due to the inner subsystem should have an amplitude of 4 mas. The orientation of the inner orbit Aa1,Aa2 can be established by frequent and precise speckle measurements of Aa,Ab. The measurements of Aa,Ab made in 2014–2015 seem to deviate from the middle orbit in a systematic way, but we could not yet use the residuals for determining the elements Ω and i of the inner orbit. The reason is that the number of measurements of Aa,Ab is still modest, leading to a cross-talk between the elements

of the middle and inner orbits. The co-planarity of those orbits thus remains hypothetical. However, the moderate eccentricity of the inner orbit implies the absence of Kozai-Lidov cycles, hence mutual inclination $\phi < 39^{\circ}$.

An attempt was made to measure the RVs of the faint components Ab and B using two-dimensional correlation, TODCOR (Zucker & Mazeh 1994). Three well-exposed spectra from TRES (JD 2455169 to 2456743) were processed using synthetic templates with effective temperatures T_e of 5750 and 4500 K. A second maximum was seen at velocities of 21.74 , 21.44 , and 25.07 km s^{-1} . All three dates are close to the node of the middle orbit Aa,Ab, so the measured velocities of the secondary, if real, correspond to a blend between Ab and B. The measurements should be repeated in a couple of years, at a different phase of the middle orbit.

4. Masses and distance

The masses and distance were determined iteratively, using photometry and orbital elements. Several assumptions are made: (i) the stars are not evolved and follow standard mass-luminosity relations for main sequence stars; (ii) the component Aa2 contributes little light in all bands, and (iii) the inner orbit Aa1,Aa2 has an inclination of

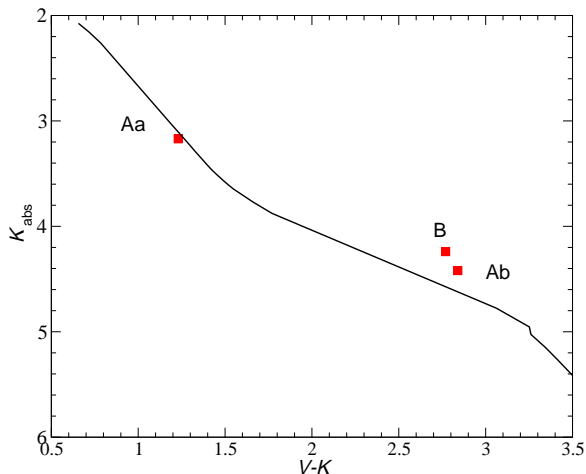


Fig. 5.— Components Aa, Ab, and B on the $(K_s, V - K_s)$ CMD with a parallax of 27.6 mas. The line shows the 1-Gyr Dartmouth isochrone with solar metallicity (Dotter et al. 2008).

57°.

Using the initial estimates of masses from the absolute *V*-band magnitudes, we determine the dynamical parallax from the middle orbit Aa,Ab, then refine the masses and other parameters. The numbers given below were obtained in the last iteration.

The mass of Aa1 is $1.14 \mathcal{M}_{\odot}$, as determined from the isochrone in Figure 5. Then the orbit of Aa1,Aa2 and the assumption (iii) lead to the mass of Aa2 of $0.32 \mathcal{M}_{\odot}$. The mass of Aa is therefore $1.46 \mathcal{M}_{\odot}$. The orbit of Aa,Ab with known inclination leads to the mass of $0.64 \mathcal{M}_{\odot}$ for Ab. The mass of A=(Aa+Ab) is therefore established at $2.10 \mathcal{M}_{\odot}$ and its semi-major axis is 5.48 AU. The semi-major axis of Aa,Ab is measured at 150 ± 2 mas and leads to the dynamical parallax of 27.4 ± 0.6 mas, i.e. a 2% accuracy on the distance. The distance is proportional to the mass sum to 1/3 power, so revision of the mass estimates would have a minor effect on the dynamical parallax.

Using the distance and photometry, we place the components Aa, Ab, and B on the color-magnitude diagram (Figure 5). The absolute magnitude of B corresponds to a main-sequence star of $0.74 \mathcal{M}_{\odot}$. However, the components Ab and B have similar luminosity, so we adopt the mass of $0.64 \mathcal{M}_{\odot}$ for B, close to the measured value for Ab. The mass sum of A+B is therefore $2.74 \mathcal{M}_{\odot}$. The orbit of A,B with a fixed period of 205 yr and the parallax of 27.4 mas corresponds to such a mass sum.

5. Discussion

The four known components of the quadruple system HD 91962 are normal dwarfs that match the standard mass-luminosity relation. We cannot exclude additional low-mass satellites revolving around Ab or B, as their RVs were not measured directly, while the constraints from the photometry and orbits are not tight enough.

The system appears to be young. White et al. (2007) measured the lithium 6707 Å line strength of 73 mÅ , axial rotation of 17 km s^{-1} , and detected chromospheric emission in a spectrum with a resolution of 16,000. Schroeder et al. (2009) confirmed the chromospheric emission, explaining the X-ray flux. The star does not belong to any known kinematic group.

No excess far-infrared emission was found with *Spitzer* (Carpenter et al. 2009). Indeed, a debris disk would not survive inside this multiple system. If the dust exists outside the orbit of A,B it would be too cold to be detectable.

All three orbits have low eccentricity. The orbits of A,B and Aa,Ab have mutual inclination of 11° . Small eccentricities imply the absence of the Kozai-Lidov cycles, hence moderate mutual orbit inclinations at all hierarchical levels. Moreover, the longitudes of periastron ω in all three orbits are also similar, showing that the lines of apsides have similar orientation. One can't help noting the similarities of the orbits while comparing the left and right parts of Figures 3 and 4.

The period ratio between the middle and inner systems is 18.97 ± 0.06 . It appears that these orbits are in a weak 1:19 resonance. The period ratio of the outer and middle systems is about 23 (it is not accurate enough to check for a resonance). The quadruple system is dynamically stable and is organized in a regular way, reminiscent of the Solar system (Figure 1). Similar eccentricities and apsidal angles, as well as the resonance, suggest that the companions interacted with each other during their formation and early dynamical evolution.

This quadruple system could originate in an isolated rotating core. Rotation prevented immediate collapse. The gas formed a massive and unstable disk which fragmented into a companion. Continuing accretion onto the companion increased its mass and caused inward migration, while dissipative gas friction maintained the low orbital eccentricity. The first companions could have merged with the central body Aa1, while other companions were formed on the periphery and migrated inwards. The process was stopped when the gas reservoir was exhausted or lost, leaving the last three surviving companions Aa2, Ab, and B. This scenario, although speculative, matches the observed properties of HD 91962.

Most quadruple systems consist of two close pairs in a 2+2 hierarchy, while the 2-tier hierarchies of 3+1 “planetary” type are less typical; they are found in about 1% of solar-type stars (Tokovinin 2014). The sample of 4847 solar-type stars within 67 pc contains only 24 multiple systems with a 3-tier hierarchy, but for none of them except HD 91962 are all three orbits known because the outer orbits have estimated periods of

several thousand years. In the current version¹ of the Multiple Star Catalog (Tokovinin 1997) we found four 3-tier hierarchies where all three orbits are known (Table 7). In those systems, the inner pairs have short orbital periods, presumably produced by inward migration. In the first system, HD 5408 (HR 266, ADS 784), the two outer orbits are nearly co-planar with periods of 83.1 yr and 4.85 yr (period ratio 17.1) and eccentricities of 0.24 and 0.22.

The architecture of HD 91962 is therefore rare, but not unique. It may belong to a class of multiple systems that evolved in a viscous disk. The distinguishing features of this class are approximate co-planarity of the orbits, moderate period ratio on the order of 20 (possibly in resonance), and small eccentricities. Other members of this class, quadruple as well as triple, may be found among known multiple systems and discovered in the future. Determination of accurate orbital elements will be essential in checking the co-planarity and resonance.

This is the case when a common visual binary turns into a unique object worth of further detailed study. The rare quadruple system HD 91962 gives interesting insights about its origin and, by extension, the origin of multiple stars in general. Further RV monitoring will help to confirm the sign of the long-term RV trend, hence the co-planarity of A,B and Aa,Ab. Precise speckle measurements of Aa,Ab with high cadence can be used to infer the orientation of the inner orbit Aa1,Aa2. This can be done even better with long-baseline interferometers. Direct resolution of the inner pair, for which we estimate $\Delta K_{Aa1,Aa2} \sim 3.8$ mag and separation on the order of 20 mas, will be difficult but not impossible. The weak signatures of B and Ab might be detectable in the high-resolution spectra with a good SNR. Such observations can prove the absence of additional close companions in this system and will provide accurate measurements of stellar masses. Future precise astrometry with *Gaia* will add new constraints.

The data used in this work were obtained at the Southern Astrophysical Research (SOAR) telescope, which is a joint project of the Ministério da Ciência, Tecnologia, e Inovação da República

Federativa do Brasil, the U.S. National Optical Astronomy Observatory, the University of North Carolina at Chapel Hill, and Michigan State University.

This work used the SIMBAD service operated by Centre des Données Stellaires (Strasbourg, France), bibliographic references from the Astrophysics Data System maintained by SAO/NASA, data products of the Two Micron All-Sky Survey (2MASS), and the Washington Double Star Catalog maintained at USNO.

REFERENCES

- Aitken, R. G. 1904, Lick Obs. Bull. 2, 139,
- Buchhave, L.A., Bizzaro, M., Latham, D. W., et al. 2014, Nature, 509, 593.
- Carpenter, J. M., Bouman, J., Mamajek, E. E. et al. 2009, ApJS, 181, 197
- Casagrande, L., Schoenrich, R., Asplund, M. et al. 2011 A&A, 530, 138
- Cutri, R. M., Skrutskie, M. F., van Dyk, S. et al. 2003 The IRSA 2MASS All-Sky Point Source Catalog. NASA/IPAC Infrared Science Archive.
- Dotter, A., Chaboyer, B., Jevremović, D. et al. 2008, ApJS, 178, 89
- Duchêne, G. & Kraus, A. 2013, ARAA, 51
- Fabrizius, C. & Makarov, V. V. 2000, A&A, 356, 141
- Horch, E. P., Ninkov, Z., & Franz, O. G., 2001, AJ, 121, 1583
- Latham, D. W. 1992, in ASP Conf. Ser. 32, Complementary Approaches to Binary and Multiple Star Research, ed. H. McAlister & W. Hartkopf (IAU Colloq. 135) (San Francisco: ASP), 110
- Latham, D. W. 1985, in IAU Colloq. 88, Stellar Radial Velocities, ed. A. G. D. Philip & D.W. Latham (Schenectady: L. Davis), 21
- Metchev S. A., Hillenbrand L. A. 2009, ApJS, 181, 62
- Popovic, G. M. 1978, Bull. Obs. Astron. Belgrade No. 129, 9

¹<http://www.ctio.noao.edu/~{atokovin}/stars/index.php>

TABLE 7
THREE-TIER HIERARCHIES WITH ALL KNOWN ORBITS IN THE MSC

HD	Sp. type	Inner	Middle	Outer
5408	B9IVn	SB2 4.24 d	SB1,VB 4.84 yr	VB 83.1 yr
9770	K4V	Ecl. 0.477 d	VB 4.56 yr	VB 123.5 yr
12376	G9V	SB2 3.08 d	VB,SB2 12.9 yr	VB 330 yr
21364	B9Vn	SB2 7.15 d	SB 145 d	VB 212 yr

Schroeder, C., Reiners, A., & Schmitt, J. H. M.
M. 2009, A&A, 493, 1099

Szentgyorgyi, A. H., & Furész, G. 2007, in The
3rd Mexico-Korea Conference on Astrophysics:
Telescopes of the Future and San Pedro Mártir,
ed. S. Kurtz, RMxAC, 28, 129

Tokovinin, A. 1997, A&AS, 124, 75

Tokovinin, A., Mason, B., & Hartkopf, W. 2010,
AJ, 139, 743

Tokovinin, A., Mason, B., & Hartkopf, W. 2014,
AJ, 147, 123

Tokovinin, A. 2014, AJ, 147, 87

van Leeuwen, F. 2007, A&A, 474, 653

White, R. J., Gabor, J. M., & Hillenbrand, L. A.
2007, AJ, 133, 252

Zucker, S. & Mazeh, T. 1994, ApJ, 420, 806

Facility: SOAR